fractal and fractional

MDPI

Article

Fractional-Order Control of Fluid Composition Conductivity

Raluca Giurgiu [1], Eva-H. Dulf [1,2,*] and Levente Kovács [3]

[1] Department of Automation, Faculty of Automation and Computer Science, Technical University of Cluj-Napoca, Memorandumului Str. 28, 400014 Cluj-Napoca, Romania
[2] Department of Environmental and Plant Protection, University of Agricultural Sciences and Veterinary Medicine Cluj-Napoca, 3-5 Manastur Str., 400374 Cluj-Napoca, Romania
[3] Physiological Controls Research Center, Óbuda University, H-1034 Budapest, Hungary
* Correspondence: eva.dulf@aut.utcluj.ro

Abstract: Dialysis refers to the procedure of removing waste products and excess fluids from the blood stream. This is the main form of treatment for both acute and chronic renal failure. The need for hemodialysis process optimization is increasing. More than 10% of adults are affected by chronic kidney disease, and it is the nineth leading cause of deaths worldwide. Critically ill patients are particularly at risk, and their mortality is significantly affected by the hemodialysis procedures. This is the reason why the design and control of the hemodialysis process is studied by many researchers. The present paper proposes a fractional-order control of the fluid composition conductivity in this process. Fractional-order PI and PID controllers are designed with different imposed performances in order to establish the best performing controller for this medical process. The proposed fractional-order controllers are compared to the classical controller's results in different real-world scenarios, including process parameter changes, flow changes, and priming sequences. The results are compared with a classical PID controller used in current clinical practice. The simulation results show the robustness and advantages of the proposed fractional-order PID controller over other controllers. These results could improve the clinical use of the hemodialysis process.

Keywords: fractional-order controller; dialysis; kidney disease; fluid composition conductivity

Citation: Giurgiu, R.; Dulf, E.-H.; Kovács, L. Fractional-Order Control of Fluid Composition Conductivity. *Fractal Fract.* **2023**, *7*, 305. https://doi.org/10.3390/fractalfract7040305

Academic Editors: Norbert Herencsar, Esteban Tlelo-Cuautle, Dumitru Baleanu and Shibendu Mahata

Received: 13 February 2023
Revised: 25 March 2023
Accepted: 29 March 2023
Published: 30 March 2023

1. Introduction

All over the world, there are patients dealing with chronic kidney disease and kidney failure, which radically change their way of life. In recent years, end-stage renal disease has become a more common disease [1]. Thus, hemodialysis comes to patients' aid; this procedure, which helps eliminate toxins and excess fluids from the bloodstream, has become the main form of treatment for these diseases. The dialysis process acts as the kidneys and performs a diffusion process to remove accumulated diffusion wastes; it also acts as an ultrafiltration process that removes excess fluids from the body. The process of dialysis is a life-prolonging treatment for patients with these diseases to allow them to live their normal lives. However, it is quite a difficult and tiring process for patients when it comes to maintaining their health in an optimal condition in between scheduled dialysis days [2]. The need for hemodialysis devices is increasing due to the fact that more than 10% of adults in developed countries are affected by chronic kidney disease (the nineth leading cause of deaths). Critically ill patients are particularly at risk, and their mortality is significantly affected by the presence or absence of renal replacement therapy.

The design and control of the hemodialysis process has been studied by many researchers, including both clinicians and engineers. A great review of this domain is presented in [3]. Currently available papers discuss issues ranging from different monitoring systems [4] to real-time detection techniques for the analysis of the key parameters of hemodialysis machines, focusing on some key parameters, such as dialysate conductivity, pH, temperature, static pulse pressure, flow, and pressure line in hemodialysis machines [5].

Most of the research deals with the problem of peristaltic pump control of hemodialysis machines, which are responsible for the fluid transfer [6]. The authors of [7] discuss a biofeedback system using noninvasive repeated measures of ionic dialysance and plasma water conductivity. Using patient measurement data, the dialysate sodium concentration is controlled by imposing a dialysate conductivity reference value. Through clinical validation, the authors prove that the proposed automatic control offers a safer operation for patients than a prescription built on an empirical or intuitive basis. The authors of [8] present a biofeedback system that influences the relative blood volume reduction by changing the ultrafiltration rate and the dialysate conductivity.

The review paper [9] examines how bio-engineering has a strong potential for defining common clinical team purposes and improving the dialysis process. The importance of a proper control system design to exclude any risk of the dialysis process is demonstrated in [10]. The necessity to individualize dialysis fluid composition to alleviate not only interdialytic symptoms but also the development of longer-term complications is demonstrated in [11]. The authors conclude that such individualization is possible only through proper equipment using automatic control.

The review [12] provides an overview of available online hemodialysis technologies, their current applications in clinical setting, and the potential for future developments in improving the care of patients with chronic kidney disease. In order to provide an efficient quality monitoring system for the hemodialysis process and to correlate with clinical outcomes, several approaches have been developed. For example, the authors of [13] present the application of urea estimation in hemodialyzed patients using artificial neural networks. The possibilities of combining system dynamics models with other health system methods, such as process-centric discrete event models, network science, and agent-based modeling, are presented in [14]. The authors prove that multi-scale, multi-level models can link physiological models, clinical practice, and health policy. Chapter [15] discusses factors that affect the hemodialysis process. The authors conclude that there are a lot of patient- and prescription-specific factors that affect the process, and understanding a patient's physiological characteristics, personal preferences, and social circumstances, coupled with the prescription of a dialysis process, will lead to the most efficient treatment for the patient. In [16], the authors analyzed how remote patient monitoring can contribute to improving patient-centered outcomes and prognosis in patients with end-stage renal disease on automated dialysis. The authors consider in their analysis the effectiveness and convenience for patients, the total amount of healthcare resource consumption, and consultation time during regular monthly visits. Their conclusions are that process automation can improve patient-centered outcomes in patients, while reducing treatment burden for both patients and medical staff. The final conclusion of the KDIGO (Kidney Disease: Improving Global Outcomes) Conference in 2018 is that many factors, such as availability of resources, reasons for starting dialysis, timing of dialysis initiation, patient education and preparedness, dialysis modality and access, as well as varied "country-specific" factors, significantly affect patient experiences and outcomes [17]. The need to move away from a "one-size-fits-all" approach to dialysis and provide more individualized care that incorporates patient goals and preferences, while still maintaining best practices for quality and safety, is becoming more and more acute, and the solution could be the use of process modeling and automated solutions.

A usual dialysis treatment lasts around four hours and is necessary three times per week. The most time-consuming activities are the overhead activities. For example, at start-up, the fluid composition control, including the concentrate control, has a very large transient period. The importance of time reduction for such activities is discussed in [18]. The author further presents the main parameter variations in the process, such as a drop of about 65% in urea concentration, the halving of serum potassium, a 25% increase in bicarbonate, and the removal of at least 2 or 3 L of water. The impact of such high variations on the body's physiology cannot be neglected. This is the reason why efforts are being

made to improve the process. In [19], a fuzzy control logic is proposed for the dialysis process. Unfortunately, no simulation or experimental results are presented.

Fractional calculus represents the generalization of integration and differentiation to an arbitrary real or a complex order. This branch of calculus has gained considerable popularity and importance nowadays mainly due to its demonstrated applications in numerous fields of science and engineering. Previous studies have discussed applications ranging from bifurcations for a fractional-order bidirectional associative memory neural network [20], or the use of a fractional-order 4D neural network incorporating two different time delays [21], to fractional-order genetic regulatory networks incorporating distributed delays and discrete delays [22]. In control engineering, Oustaloup first introduced the notion of fractional order, developed the "Commande Robuste d'Ordre Non Entier (CRONE)" controller [23], and highlighted the advantages of this calculus. The generalization of the classical, most commonly used PID controllers is facilitated by Podlubny, who introduced the so-called fractional-order $PI^{\lambda}D^{\mu}$ controllers [24]. Since then, many researchers have focused on the design problem of fractional-order controllers, especially to enhance the robustness and performance of these control systems and to apply these advantages in different applications [25–29], including those in medical field [30].

This paper highlights the benefits offered by fractional control in the medical field, which can provide a solution to improving automatic control in the hemodialysis process. To the best of our knowledge, no such control solution has been proposed in the literature. The proposed control is based on optimizing the conductivity of the dialysis fluid, which is composed of two concentrates and is an important parameter, along with pH, temperature, and flow rate. Fractional-order PI and PID controllers are designed with different imposed performances used in clinical practice in order to establish the best performing controller for this medical process. The proposed fractional-order controllers are compared with the classical controller's results in different scenarios, including process parameter changes, flow changes, and priming sequences. These results could improve the clinical use of the hemodialysis process.

This paper is structured in four sections. After this short introductory part, Section II presents the used process model. Section III describes the design of the fractional-order controllers. The results are discussed in Section IV. Finally, this work ends with some concluding remarks.

2. Materials and Methods

A schematic diagram of fluid preparation in a dialysis machine is presented in Figure 1.

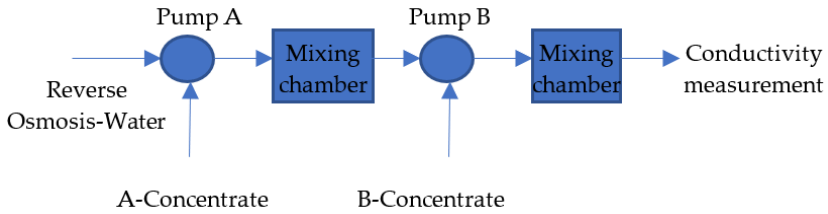

Figure 1. Simplified schematic diagram of fluid preparation.

Concentrate A is a mixture of electrolytes to match a patient's blood content. It has very good conductivity, and its solubility in water does not depend on temperature. Concentrate B includes bicarbonate and acts as a pH buffer. Its solubility is temperature dependent, which implies modeling complications. The two concentrates cannot be added at the same point in the fluid path due to the risk of bicarbonate precipitation. Both concentrates A and B are available as a solution or as a dry product to which the machine adds water. The corresponding pumps are reciprocating pumps powered by stepper motors. They imply a constant volumetric flow rate for each rotation. Thus, a disturbance is added to the output. A mixing chamber is added, which is separated into two small chambers by a divider. After the last mixing chamber, a conductivity measuring cell is used to measure the feedback signal.

Assuming a homogeneous mixture and using the mass conservation laws, the process model can be obtained as follows [31]:

$$H_f(s) = \left[\frac{\frac{Q^4 K_A}{(V_1 V_2 V_3 V_4)}}{\left(s+\frac{Q}{V_1}\right)\left(s+\frac{Q}{V_2}\right)\left(s+\frac{Q}{V_3}\right)\left(s+\frac{Q}{V_4}\right)} e^{-s\tau_A}, \ \frac{\frac{Q^2 K_B}{V_3 V_4}}{\left(s+\frac{Q}{V_3}\right)\left(s+\frac{Q}{V_4}\right)} e^{-s\tau_B} \right] \begin{bmatrix} Pu_A \\ Pu_B \end{bmatrix} \quad (1)$$

where Q is the main fluid flow; $V_{1,2,3,4}$ are the volumes of each sub-chamber; K_A and K_B are the steady state gains of A- and B-concentrate, respectively; τ_A and τ_B are the delay time from the point of injection to the point of measurement; and Pu_A and Pu_B are the volumetric flow of the concentrates. For the present research, the numerical values are as follows: Q = 500 [mL/min]; V_1 = 0.0399 [L]; V_2 = 0.0295 [L]; V_3 = 0.0384 [L]; V_4 = 0.0216 [L]; K_A = 0.8431; K_B = 0.1328; τ_A = 4.51 [s]; and τ_B = 2.04 [s].

The continuous transfer function of a fractional-order PID controller has the following general form [24]:

$$H_C(s) = K_P\left(1 + \frac{K_i}{s^\lambda} + K_d s^\mu\right) \quad (2)$$

where $0 < \lambda < 1$ and $0 < \mu < 1$ are the fractional orders of integration and differentiation, respectively; K_P is the proportional gain; and K_i and K_d are the integral and derivative gains, respectively. Such controllers have two more degrees of freedom (the fractional orders of integration λ and of differentiation μ) in comparison with a classical PID controller. This flexibility comes with important advantages, such as better closed-loop performance, disturbance rejection capabilities, improved control of time delay systems, and increased robustness. The fractional-order derivative/integral can be described by the definitions listed below [29].

The Riemann–Liouville definition:

$$D_c^{-\alpha} f(t) = \frac{1}{\Gamma(\alpha)} \int_c^t (t-\tau)^{\alpha-1} f(\tau) d\tau, \ t > c, \ \alpha \in R^+$$

where $\Gamma(\alpha) = \int_0^\infty t^{n-1} e^{-t} dt$ is the Euler's Gamma function, which is a generalization of a fractional derivative, and $n \in R^+$ is an extension of the fractional integral.

The Caputo definition:

$${}_c D^\alpha f(t) = \frac{1}{\Gamma(m-\alpha)} \int_c^t \frac{f^{(m)}(\tau)}{(t-\tau)^{\alpha-m+1}} d\tau, \ m-1 < \alpha < m, \ m \in N$$

The Grünwald–Letnikov definition of the fractional-order derivative:

$${}_{GL} D^\alpha f(t) = \sum_{k=0}^m \frac{f^{(k)}(0^+) t^{k-\alpha}}{\Gamma(m+1-\alpha)} + \frac{1}{\Gamma(m+1-\alpha)} \int_0^t (t-\tau)^{m-\alpha} f^{(m+1)}(\tau) d\tau, \ m > \alpha - 1$$

The fractional integration and differentiation in frequency domain are expressed by the Euler equations:

$$s^\mu = (j\omega)^\mu = \omega^\mu \left(\cos\frac{\mu\pi}{2} + j \sin\frac{\mu\pi}{2}\right); \quad (3)$$

$$s^{-\lambda} = (j\omega)^{-\lambda} = \omega^{-\lambda} \left(\cos\frac{\lambda\pi}{2} - j \sin\frac{\lambda\pi}{2}\right) \quad (4)$$

The imaginary and real parts of the controller are defined as follows:

$$Im = K_p \left(K_d \omega^\mu \sin\frac{\mu\pi}{2} - K_i \omega^{-\lambda} \sin\frac{\lambda\pi}{2}\right) \quad (5)$$

$$Re = K_p\left(1 + K_i\omega^{-\lambda}\cos\frac{\lambda\pi}{2} + K_d\omega^{\mu}\cos\frac{\mu\pi}{2}\right) \tag{6}$$

In frequency domain, the magnitude, phase, and phase derivative of the fractional-order PI controller can be expressed as

$$|H_C(j\omega_{gc})| = \sqrt{Im^2 + Re^2}\,,\ \angle H_C(j\omega_{cg}) = a\tan\left(\frac{Im}{Re}\right),\ \phi = \frac{d\angle H_c(j\omega_{cg})}{d\omega}$$

or expressed with all the terms of the following equations:

$$|H_C(j\omega)| = \sqrt{\left(K_p + \frac{K_p}{T_i}\omega^{-\lambda}\cos\frac{\lambda\pi}{2}\right)^2 + \left(\frac{K_p}{T_i}\omega^{-\lambda}\sin\frac{\lambda\pi}{2}\right)^2} \tag{7}$$

$$\angle H_C(j\omega) = a\tan\left(\frac{\frac{K_p}{T_i}\omega^{-\lambda}\sin\frac{\lambda\pi}{2}}{K_p + \frac{K_p}{T_i}\omega^{-\lambda}\cos\frac{\lambda\pi}{2}}\right) \tag{8}$$

$$\frac{d\angle H_c(j\omega)}{d\omega} = \frac{\lambda T_i\omega^{\lambda-1}\sin\frac{\lambda\pi}{2}}{T_i^2\omega^{2\lambda}\sin^2\frac{\lambda\pi}{2} + \left(T_i\omega^{\lambda}\cos\frac{\lambda\pi}{2} + 1\right)^2} \tag{9}$$

The same equations for the fractional-order PID controller are as follows:

$$|H_C(j\omega)| = K_p\sqrt{K_d\omega^{\mu}\left(\sin\frac{\mu\pi}{2} + \cos\frac{\mu\pi}{2}\right) + \left(\omega^{-\lambda}K_i\cos\frac{\lambda\pi}{2} + 1\right)^2 - \left(\omega^{-\lambda}K_i\sin\frac{\lambda\pi}{2}\right)^2} \tag{10}$$

$$\angle H_C(j\omega) = a\tan\frac{K_d\omega^{\mu}\sin\frac{\mu\pi}{2} - K_i\omega^{-\lambda}\sin\frac{\lambda\pi}{2}}{1 + K_i\omega^{-\lambda}\cos\frac{\lambda\pi}{2} + K_d\omega^{-\mu}\cos\frac{\mu\pi}{2}} \tag{11}$$

$$\frac{d\angle H_c(j\omega)}{d\omega} = \frac{\omega^{\lambda-1}\left(K_i\lambda\sin\frac{\pi\lambda}{2} + K_dK_i\lambda\omega^{\mu}\sin\frac{\pi(\lambda+\mu)}{2} + K_dK_i\mu\omega^{\mu}\sin\frac{\pi(\lambda+\mu)}{2} + K_d\mu\omega^{\lambda+\mu}\sin\frac{\pi\mu}{2}\right)}{\omega^{2\lambda} + K_i^2 + K_d^2\omega^{2(\lambda+\mu)} + 2K_i\omega^{\lambda}\cos\frac{\pi\lambda}{2} + 2K_d\omega^{2\lambda+\mu}\cos\frac{\pi\mu}{2} + 2K_dK_i\omega^{\lambda+\mu}\cos\frac{\pi(\lambda+\mu)}{2}} \tag{12}$$

After imposing the phase margin (PM), the gain crossover frequency (ω_{cg}), and the iso-damping property as the performance measures for the open-loop system, the equations for establishing the controller parameters become the following:

$$|H_C(j\omega_{-\pi})| = \sqrt{Im^2 + Re^2} = \frac{GM}{\left|H_f(j\omega_{-\pi})\right|}\,, \tag{13}$$

$$\angle H_C(j\omega_{cg}) = a\tan\left(\frac{Im}{Re}\right) = PM - \angle H_f(j\omega_{cg}) \tag{14}$$

$$\frac{d\angle H_c(j\omega_{gc})\cdot H_c(j\omega_{gc})}{d\omega} = 0 \tag{15}$$

where ω_{cg} is the gain crossover frequency; $\omega_{-\pi}$ is the phase crossover frequency; GM is the gain margin; and H_f stands for the process model. When replacing Equations (13)–(15) with the magnitude, phase, and phase derivative equations of the fractional-order PI (7)–(9) and PID controllers (10)–(12), it results in a nonlinear equation system from which the controller parameters can be obtained. In the present work, the Multi-objective Genetic Algorithm (MOGA) is used to solve this nonlinear system, as detailed in [32].

In order to compare the advantages introduced by the fractional-order controllers, a classical, integer-order controller is designed, replacing the fractional-order integrator and differentiator with 1.

3. Results

As the first experiment, a classical PI controller is designed for the concentrate A, omitting the derivative terms in Equations (5)–(8) and using the integration order of one (integer-order PI controller). The imposed performances—inspired by the range of values reported in the literature for clinical practice [9,13–15,17–19]—and the resulting fractional-order PI controller parameters are presented in Table 1.

Table 1. The imposed performances and the resulting integer-order PI controller parameters.

Controller	PM [°]	ω_{gc} [rad/s]	K_p	K_i
H_{R_1}	45	0.05	0.1	1.75
H_{R_2}	65	0.06	1.012	16.86
H_{R_3}	62	0.03	0.12	3.23

The resulting Bode diagrams are plotted in Figures 2–4, highlighting the fulfillment of the imposed performances.

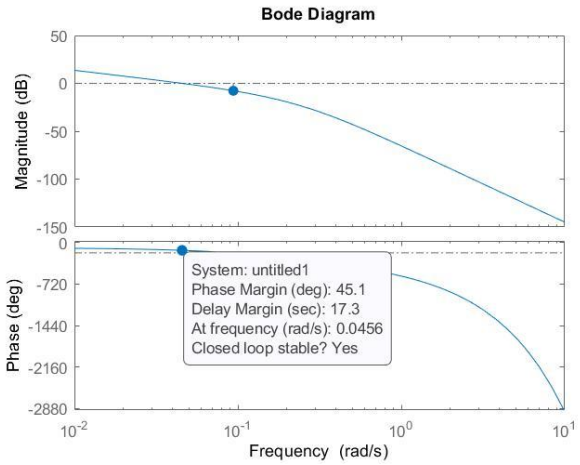

Figure 2. Bode diagram of the open-loop system for the first designed PI controller.

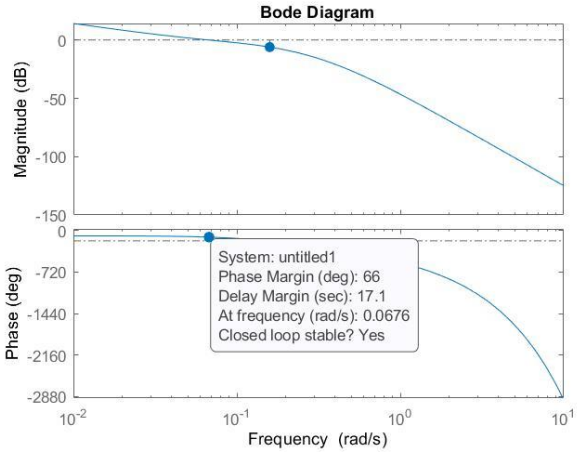

Figure 3. Bode diagram of the open-loop system for the second designed PI controller.

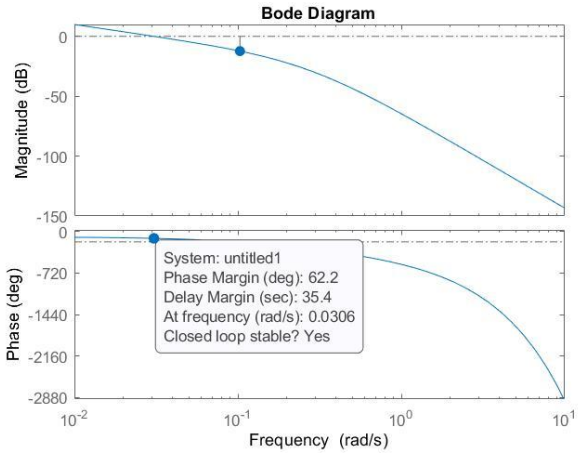

Figure 4. Bode diagram of the open-loop system for the third designed PI controller.

The corresponding step responses of the closed-loop system are plotted in Figure 5.

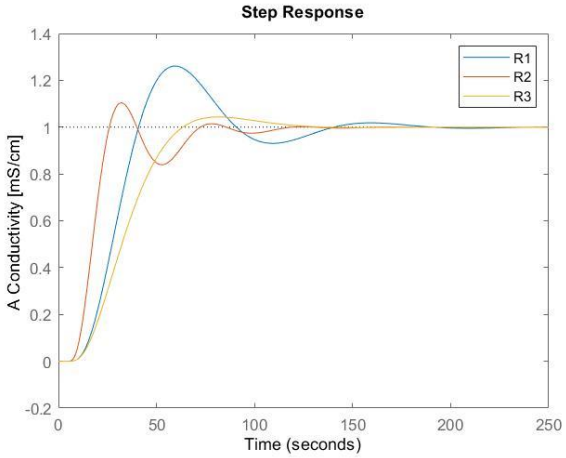

Figure 5. Step responses of the closed-loop system for the three designed PI controllers.

The second experiment involved the design of a fractional-order PI (FO-PI) controller, using the same performance measures as in the integer-order case and, as an additional performance measure, the iso-damping property in Equation (9). The resulting FO-PI controller parameters are presented in Table 2.

Table 2. The imposed performances and the resulting FO-PI controller parameters.

Controller	PM [°]	ω_{gc} [rad/s]	K_p	K_i	λ
H_{G_1}	45	0.05	0.08	10.68	0.89
H_{G_2}	65	0.06	0.79	13.52	0.93
H_{G_3}	62	0.03	0.02	15.48	0.91

Using the Matlab FOMCON Toolbox [33], the corresponding Bode plots are generated and shown in Figures 6–8. For the fractional-order controller, the Oustaloup Recursive Approximation method is used [34], within a frequency band [0.01, 10] rad/s and with an order N = 10.

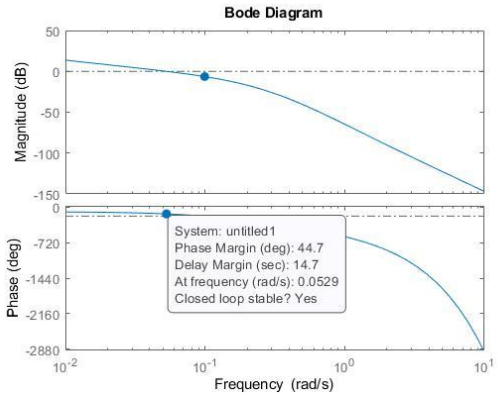

Figure 6. Bode diagram of the open-loop system for the first designed FO-PI controller.

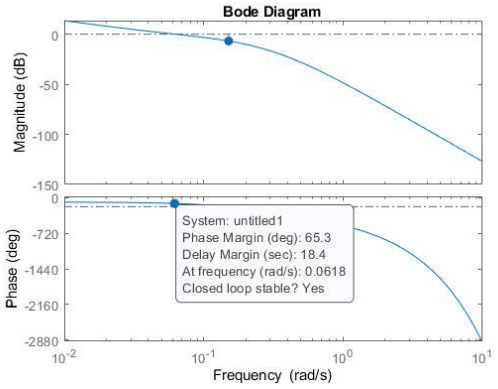

Figure 7. Bode diagram of the open-loop system for the second designed FO-PI controller.

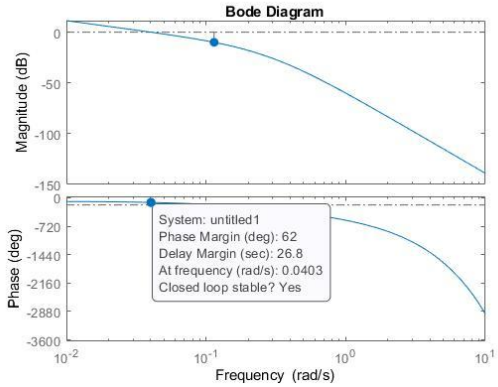

Figure 8. Bode diagram of the open-loop system for the third designed FO-PI controller.

The corresponding step responses are plotted in Figure 9. It can be seen that all performances are the same for the cases of the integer-order PI and FO-PI, which have been imposed with the same performances, with the exception of the additional performance, the iso-damping frequency.

The third experiment is the design of the FO-PID controller using Equations (4)–(8). The imposed performance measures are the same as in the previous experiments. The resulting controller parameters are highlighted in Table 3.

The obtained Bode diagrams are presented in Figures 10–12. The step responses of the closed-loop system with the FO-PID controller are presented in Figure 13.

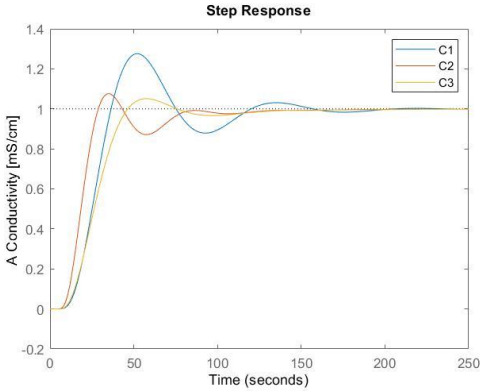

Figure 9. Step responses of the closed-loop system for the three designed FO-PI controllers.

Table 3. The imposed performances and the resulting FO-PID controller parameters.

Controller	PM [°]	ω_{gc} [rad/s]	K_p	K_i	λ	K_d	μ
H_{G_1}	45	0.05	0.08	0.1	0.89	0.6	0.55
H_{G_2}	65	0.06	0.79	0.075	0.93	0.09	0.9
H_{G_3}	62	0.03	0.1	0.05	0.95	0.1	0.58

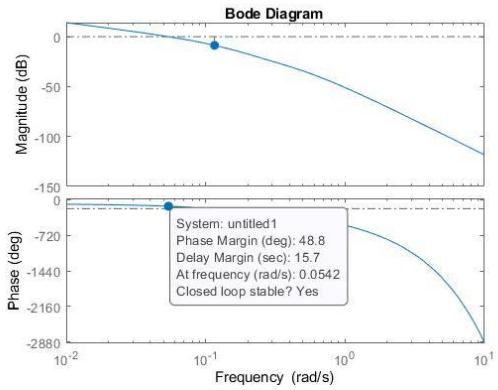

Figure 10. Bode diagram of the open-loop system for the first designed FO-PID controller.

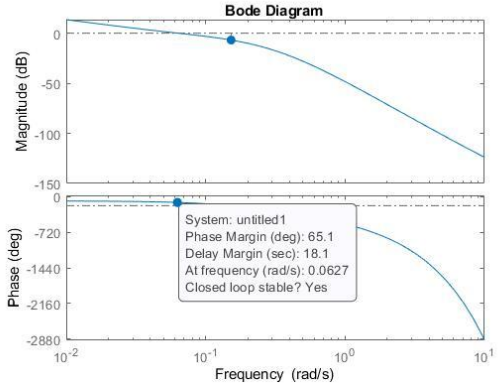

Figure 11. Bode diagram of the open-loop system for the second designed FO-PID controller.

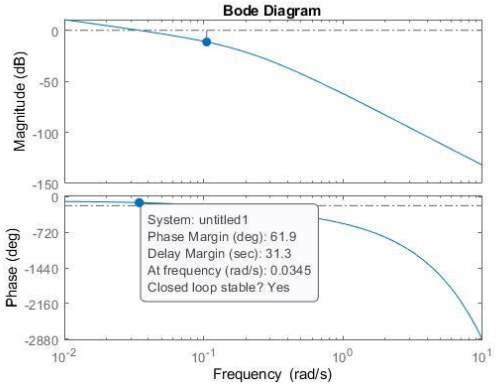

Figure 12. Bode diagram of the open-loop system for the third designed FO-PID controller.

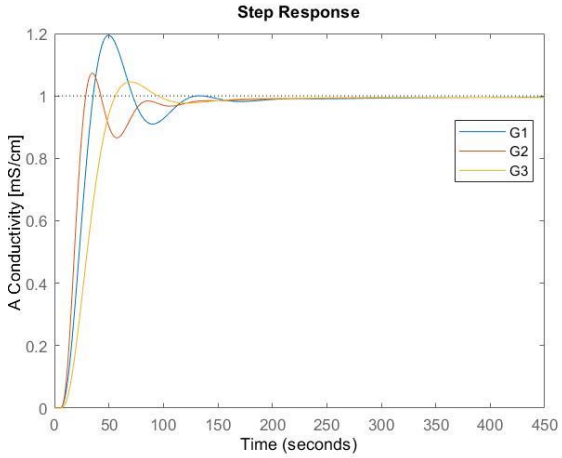

Figure 13. Step responses of the closed-loop system for the three designed FO-PID controllers.

The robustness analysis of the resulting controllers is the last step in this research. The process parameters are modified with +/−2% changes, which can occur in practice due to patient particularities and operation changes. With each designed controller, the Bode diagrams and step responses are simulated to establish performance variations. The resulting phase margins, gain crossover frequencies, settling time, and overshoot are established. The obtained results, in comparison with the initial values, for the nominal parameters are shown in Tables 4 and 5.

Table 4. Performance results for +2% parameter changes in the process.

Controller	Results with Nominal Parameters				Performance Changes with +2% Parameter Changes			
	PM [°]	ω_{gc} $\left[\frac{\text{rad}}{\text{s}}\right]$	t_s [s]	σ [%]	PM [°]	ω_{gc} $\left[\frac{\text{rad}}{\text{s}}\right]$	t_s [s]	σ [%]
PI	62	0.03	136	4.5	1.8	0.0540	1	4.03
FO-PI					0	0.0103	0.5	0.70
FO-PID					0.1	0.0045	0	0.57

The step responses of the closed-loop system for all three types of controllers—integer-order PI, FO-PI, and FO-PID—are presented in Figures 14 and 15. It can be noticed that the most robust controller is the FO-PID. For example, the overshoot for the classical integer-order controller changes by 4.03% in the case of +2% plant parameter changes, but the FO-PID has only 0.57% overshoot changes, followed by the FO-PI with 0.7% overshoot

changes. The same good robustness can be ascertained in the case of −2% parameter changes in the process.

Table 5. Performance results for −2% parameter changes in the process.

Controller	Results with Nominal Parameters				Performance Changes with −2% Parameter Changes			
	PM [°]	ω_{gc} $\left[\frac{\text{rad}}{\text{s}}\right]$	t_s [s]	σ [%]	PM [°]	ω_{gc} $\left[\frac{\text{rad}}{\text{s}}\right]$	t_s [s]	σ [%]
PI	62	0.03	136	4.5	2.8	0.0640	6	2.80
FO-PI					0	0.0103	2	1.88
FO-PID					0.1	0.0045	1	0.70

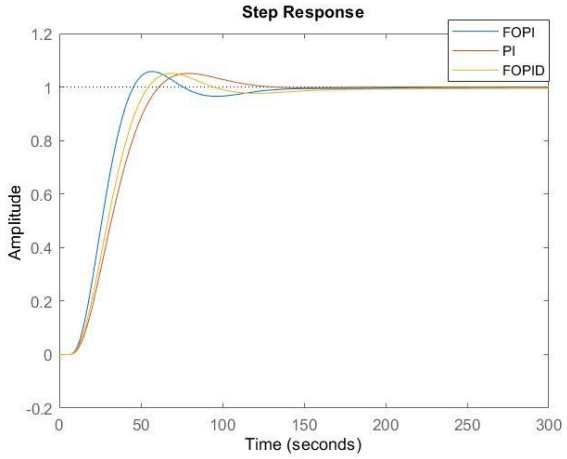

Figure 14. Step responses of the closed-loop system for the integer-order PI, FO-PI, and FO-PID controllers in the case of +2% process changes.

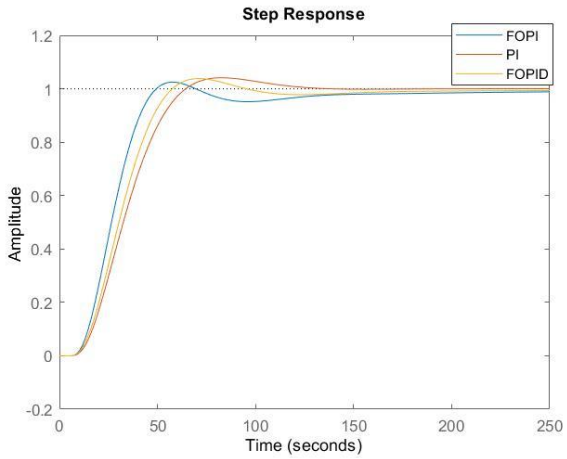

Figure 15. Step responses of closed-loop system for the integer-order PI, FO-PI, and FO-PID controllers in the case of −2% process changes.

The performance changes in the frequency responses are plotted in Figures 16 and 17.

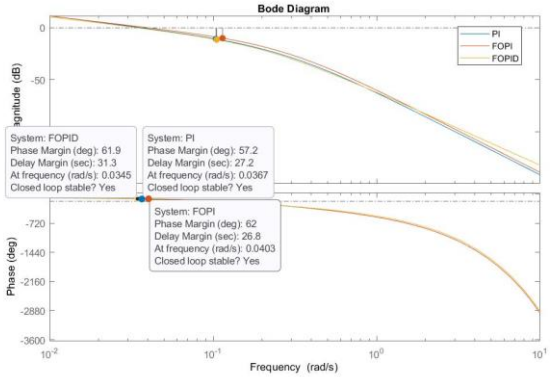

Figure 16. Bode diagrams of the open-loop system for the integer-order PI, FO-PI, and FO-PID controllers in the case of +2% process changes.

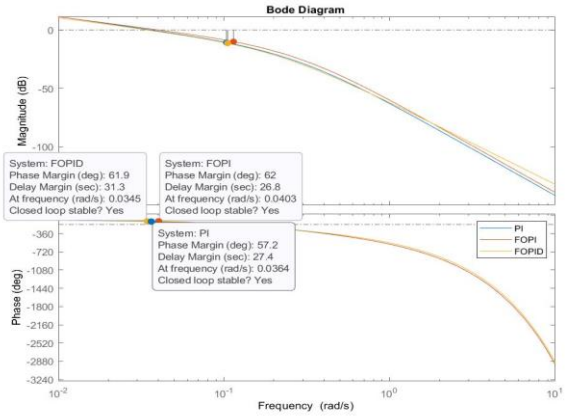

Figure 17. Bode diagrams of the open-loop system for the integer-order PI, FO-PI, and FO-PID controllers in the case of −2% process changes.

As the first clinical use scenario, we also simulated the case when noisy output is used as the feedback. A white noise is applied on the measured output, with 0.1 power spectral density. The step responses of the closed-loop system for the integer-order controller and the fractional-order PI and PID controllers are presented in Figure 18. It can be noticed the good noise rejection of the two fractional-order controllers.

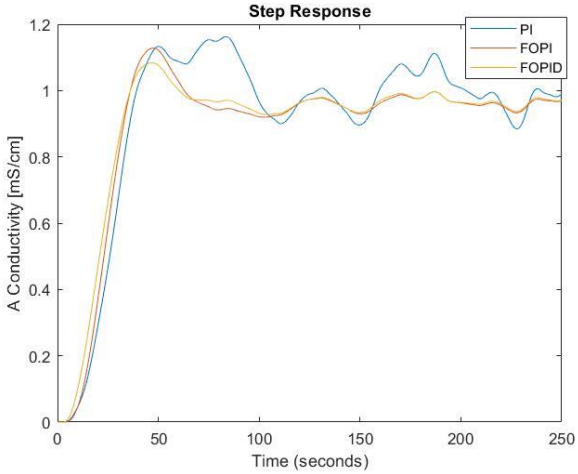

Figure 18. Step responses of the closed-loop system for the integer-order PI, FO-PI, and FO-PID controllers in the case of noise.

As the second clinical use scenario, we simulated the cases when main flow changes are necessary in the treatment. Figure 19 presents such a case, when the main flow is changed from 2.5 unity to 9.5 unity. The blue curve represents the output using the classical integer-order controller, while the red and yellow curves are the outputs using the fractional-order PI and PID controllers. The adaptation of the fractional-order controllers is way superior to the integer-order controller.

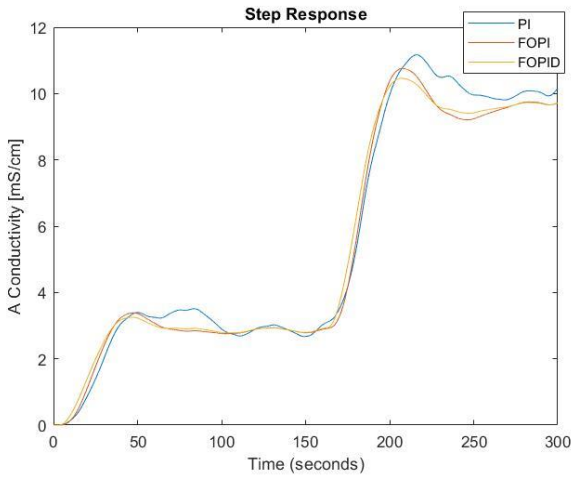

Figure 19. Step responses of the closed-loop system for the integer-order PI, FO-PI, and FO-PID controllers in the case of main flow changes.

Another issue related to clinical robustness testing is the priming sequences. When a treatment begins, the dialysis equipment is empty. The pick-up tubes must be filled with the proper concentrate. The priming consists of running the pumps until a proper conductivity is achieved. Figure 20 presents such a simulated scenario, highlighting once again the advantages of the fractional-order controllers, which show a smaller priming time in comparison to the integer-order PI controller.

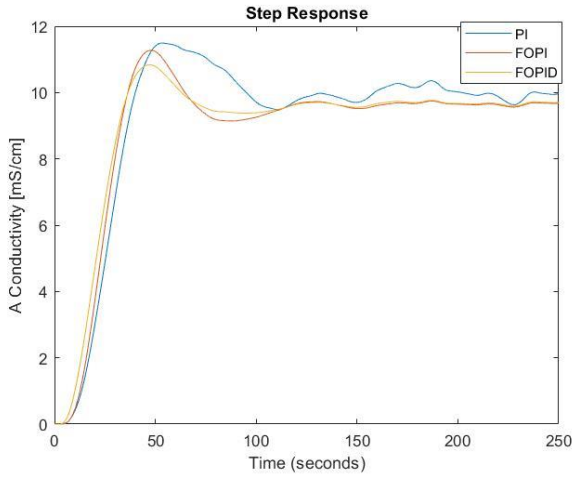

Figure 20. Step responses of the closed-loop system for the integer-order PI, FO-PI, and FO-PID controllers in the case of priming sequences.

4. Conclusions

The conductivity control based on the mathematical model of concentrates in a hemodialysis machine is discussed in the present research. This work aimed to improve the control system to help optimize dialysate performances for people with chronic kidney disease. Three types of controllers were implemented: a classical integer-order PI controller, which is used in current clinical practice; a fractional-order PI controller; and a

fractional-order PID controller. The additional degrees of freedom were used for robustness issues. This robustness was tested by +/−2% process parameter changes, noise rejection, input changes, and priming sequences. The obtained results prove the superiority of the fractional-order controllers. Using such controllers in clinical practice could improve the efficiency of the hemodialysis process.

Future works include an extension of the fractional-order controller design for the entire hemodialysis process and practical implementation.

Author Contributions: Conceptualization, E.-H.D. and R.G.; methodology, E.-H.D., L.K. and R.G.; software, R.G.; validation, E.-H.D. and R.G; formal analysis, L.K.; writing—original draft preparation, R.G.; writing—review and editing, E.-H.D.; supervision, L.K. All authors have read and agreed to the published version of the manuscript.

Funding: This work was supported by a grant from the Ministry of Research, Innovation and Digitization, CNCS-UEFISCDI, project number PN-III-P4-PCE-2021-0750, within PNCDI III.

Data Availability Statement: Data and methods used in the research are presented in sufficient detail in the manuscript so that other researchers can replicate our work.

Conflicts of Interest: The authors declare no conflict of interest.

References

1. Kalantar-Zadeh, K.; Jafar, T.H.; Nitsch, D.; Neuen, B.L.; Perkovic, V. Chronic kidney disease. *Lancet* **2021**, *398*, 786–802. [CrossRef] [PubMed]
2. Romagnani, P.; Remuzzi, G.; Glassock, R.; Levin, A.; Jager, K.J.; Tonelli, M.; Massy, Z.; Wanner, C.; Anders, H.-J. Chronic kidney disease. *Nat. Rev. Dis. Prim.* **2017**, *3*, 17088. [CrossRef] [PubMed]
3. Vanholder, R. Future Directions for Dialysis. *Kidney Dial.* **2022**, *2*, 153–162. [CrossRef]
4. Zainol, M.F.; Farook, R.S.M.; Hassan, R.; Halim, A.H.A.; Rejab, M.R.A.; Husin, Z. A New IoT Patient Monitoring System for Hemodialysis Treatment. In Proceedings of the 2019 IEEE Conference on Open Systems (ICOS), Pulau Pinang, Malaysia, 19–21 November 2019.
5. Shi, H.-Y.; Wu, X.-Q.; Wang, L.-H.; Li, L. Design of Real-time Detection System for Hemodialysis Machine Operating Parameters. *J. Appl. Sci. Eng. Innov.* **2018**, *5*, 113–116.
6. Klespitz, J.; Takács, M.; Kovács, L. Application of Fuzzy Logic in Hemodialysis Equipment. In Proceedings of the IEEE 18th International Conference on Intelligent Engineering Systems INES 2014, Tihany, Hungary, 3–5 July 2014.
7. Bosetto, A.; Bene, B.; Petitclerc, T. Sodium management in dialysis by conductivity. *Adv. Ren. Replace. Ther.* **1999**, *6*, 243–254. [CrossRef]
8. Locatelli, F.; Buoncristiani, U.; Canaud, B.; Köhler, H.; Petitclerc, T.; Zucchelli, P. Haemodialysis with on-line monitoring equipment: Tools or toys? *Nephrol. Dial. Transplant.* **2005**, *20*, 22–33. [CrossRef]
9. Kliger, A.S. Maintaining safety in the dialysis facility. *Clin. J. Am. Soc. Nephrology* **2015**, *10*, 688–695. [CrossRef]
10. Polaschegg, H.D. Red Blood Cell Damage from Extracorporeal Circulation in Hemodialysis. In *Seminars in Dialysis*; Blackwell Publishing Ltd.: Oxford, UK, 2009; Volume 22, pp. 524–531.
11. Hoenich, N.; Thijssen, S.; Kitzler, T.; Levin, R.; Ronco, C. Impact of water quality and dialysis fluid composition on dialysis practice. *Blood Purif.* **2008**, *26*, 6–11. [CrossRef]
12. Canaud, B.; Granger, A.; Chenine-Khoualef, L.; Patrier, L.; Morena, M.; Leray-Moragués, H. On-Line Hemodialysis Monitoring: New Tools for Improving Safety, Tolerance and Efficacy. In *Modeling and Control of Dialysis Systems. Studies in Computational Intelligence*; Azar, A., Ed.; Springer: Berlin/Heidelberg, Germany, 2013; Volume 405. [CrossRef]
13. Fernández, E.A.; Valtuille, R.; Balzarini, M. Artificial Neural Networks Applications in Dialysis. In *Modeling and Control of Dialysis Systems. Studies in Computational Intelligence*; Azar, A., Ed.; Springer: Berlin/Heidelberg, Germany, 2013; Volume 405. [CrossRef]
14. McDonnell, G.; Azar, A.T.; White, J.C. Renal System Dynamics Modeling. In *Modeling and Control of Dialysis Systems. Studies in Computational Intelligence*; Azar, A., Ed.; Springer: Berlin/Heidelberg, Germany, 2013; Volume 405. [CrossRef]
15. To, K.C.; Brimble, K.S. Factors Affecting Peritoneal Dialysis Dose. In *Modeling and Control of Dialysis Systems. Studies in Computational Intelligence*; Azar, A., Ed.; Springer: Berlin/Heidelberg, Germany, 2013; Volume 405. [CrossRef]
16. Uchiyama, K.; Morimoto, K.; Washida, N.; Kusahana, E.; Nakayama, T.; Itoh, T.; Kasai, T.; Wakino, S.; Itoh, H. Effects of a remote patient monitoring system for patients on automated peritoneal dialysis: A randomized crossover controlled trial. *Int. Urol. Nephrol.* **2022**, *54*, 2673–2681. [CrossRef]
17. Chan, C.T.; Blankestijn, P.J.; Dember, L.M.; Gallieni, M.; Harris, D.C.; Lok, C.E.; Mehrotra, R.; Stevens, P.E.; Wang, A.Y.M.; Cheung, M.; et al. Dialysis initiation, modality choice, access, and prescription: Conclusions from a Kidney Disease: Improving Global Outcomes (KDIGO) Controversies Conference. *Kidney Int.* **2019**, *96*, 37–47. [CrossRef]
18. Azar, A.T. *Modeling and Control of Dialysis Systems*; Springer: Berlin/Heidelberg, Germany, 2013; Volume 1.

19. Giove, S.; Azar, A.T.; Nordio, M. Fuzzy Logic Control for Dialysis Application. In *Modeling and Control of Dialysis Systems. Studies in Computational Intelligence*; Azar, A., Ed.; Springer: Berlin/Heidelberg, Germany, 2013; Volume 405. [CrossRef]
20. Huang, C.; Wang, J.; Chen, X.; Cao, J. Bifurcations in a fractional-order BAM neural network with four different delays. *Neural. Netw.* **2021**, *141*, 344–354. [CrossRef]
21. Xu, C.; Mu, D.; Liu, Z.; Pang, Y.; Liao, M.; Aouiti, C. New insight into bifurcation of fractional-order 4D neural networks incorporating two different time delays. *Commun. Nonlinear Sci. Numer. Simul.* **2023**, *118*, 107043. [CrossRef]
22. Li, P.; Li, Y.; Gao, R.; Xu, C.; Shang, Y. New exploration on bifurcation in fractional-order genetic regulatory networks incorporating both type delays. *Eur. Phys. J. Plus* **2022**, *137*, 598. [CrossRef]
23. Oustaloup, A.; Sabatier, J.; Lanusse, P. From Fractional Robustness to CRONE Control. In *Fractional Calculus and Applied Analysis*; Springer: Berlin/Heidelberg, Germany, 1999; Volume 2, pp. 1–30.
24. Podlubny, I. Fractional-order systems and $PI^{\lambda}D^{\mu}$ controllers. *IEEE Trans. Autom. Control.* **1999**, *44*, 208–214. [CrossRef]
25. Dulf, E.H. Simplified fractional order controller design algorithm. *Mathematics* **2019**, *7*, 1166. [CrossRef]
26. Dulf, E.H.; Dulf, F.V.; Muresan, C.I. Fractional model of the cryogenic (13C) isotope separation column. *Chem. Eng. Commun.* **2015**, *202*, 1600–1606. [CrossRef]
27. Chen, P.; Ying, L. An analytical synthesis of fractional order $PI^{\lambda}D^{\mu}$ controller design. *ISA Trans.* **2022**, *131*, 124–136. [CrossRef]
28. Oziablo, P.; Mozyrska, D.; Wyrwas, M. Fractional-variable-order digital controller design tuned with the chaotic yellow saddle goatfish algorithm for the AVR system. *ISA Trans.* **2022**, *125*, 260–267. [CrossRef]
29. Dulf, E.H.; Șușcă, M.; Kovács, L. Novel Optimum Magnitude Based Fractional Order Controller Design Method. *IFAC-PapersOnLine* **2018**, *51*, 912–917. [CrossRef]
30. Hegedus, E.T.; Birs, I.R.; Ghita, M.; Muresan, C.I. Fractional-Order Control Strategy for Anesthesia–Hemodynamic Stabilization in Patients Undergoing Surgical Procedures. *Fractal Fract.* **2022**, *6*, 614. [CrossRef]
31. Fällman, M. Model-Based Conductivity Control of Fluid Composition. MSc Thesis, Department of Automatic Control, Lund University, 2016.
32. Paducel, I.; Safirescu, C.O.; Dulf, E.H. Fractional Order Controller Design for Wind Turbines. *Appl. Sci.* **2022**, *12*, 8400. [CrossRef]
33. Tepljakov, A. FOMCON Toolbox for MATLAB. Available online: https://github.com/extall/fomcon-matlab/releases/tag/v1.50.3 (accessed on 19 October 2022).
34. Oustaloup, A.; Levron, F.; Mathieu, B.; Nanot, F.M. Frequency-band complex noninteger differentiator: Characterization and synthesis. *IEEE Trans. Circuits Syst. I: Fundam. Theory Appl.* **2020**, *47*, 25–39. [CrossRef]